

Magnetic gas sensing using a dilute magnetic semiconductor

A. Punnoose,^{a)} K. M. Reddy, J. Hays, and A. Thurber
Department of Physics, Boise State University, Boise, Idaho 83725

M. H. Engelhard
Environmental Molecular Sciences Laboratory, Pacific Northwest National Laboratory, Richland, Washington 99352

(Received 23 March 2006; accepted 17 July 2006; published online 14 September 2006)

The authors report on a magnetic gas sensing methodology to detect hydrogen using the ferromagnetic properties of a nanoscale dilute magnetic semiconductor $\text{Sn}_{0.95}\text{Fe}_{0.05}\text{O}_2$. This work demonstrates the systematic variation of saturation magnetization, coercivity, and remanence of $\text{Sn}_{0.95}\text{Fe}_{0.05}\text{O}_2$ with the hydrogen gas flow rate, thus providing clear experimental evidence of the concept of magnetic gas sensing (using the magnetic property of a material as a gas sensing parameter). Based on the results of using hydrogen as an example for reducing gases, it is believed that any reducing gas capable of changing the oxygen stoichiometry of $\text{Sn}_{0.95}\text{Fe}_{0.05}\text{O}_2$ can be detected using this method. Furthermore, this method presents an alternative gas sensing technology without the use of the electrical contacts. © 2006 American Institute of Physics.

[DOI: 10.1063/1.2349284]

Conventional oxide-semiconductor-based solid state gas sensors employ changes in their electrical properties with oxygen stoichiometry to detect reducing gases such as hydrogen.^{1,2} Detection of leaks in hydrogen storage vessels in mobile systems, such as hydrogen-powered cars and fuel supply lines in future automobile technology, requires the development of more efficient, highly portable, and sensitive hydrogen sensors. Conventional semiconductor gas sensors suffer from low sensitivity and serious difficulties associated with complex electrical contacts on micro- and nanoscale gas sensing systems, especially when exposed to reactive chemical environments and when employed in mobile components. Since oxygen vacancies are primarily produced on the surface of the particles/films, a means to significantly improve the gas sensitivity would be to develop methods that utilize the high surface area of nanoparticles. Unfortunately, powder samples cannot be used in the conventional electrical-property-based sensing methods since stable electrical contacts are extremely difficult to make on powder particles, especially in mobile applications.

Here we show that the ferromagnetic (FM) properties of a nanoscale dilute magnetic semiconductor (DMS), $\text{Sn}_{0.95}\text{Fe}_{0.05}\text{O}_2$ powder,^{3,4} can be used to detect hydrogen without electrical contacts. It has been predicted theoretically^{5,6} and demonstrated experimentally^{3,4,7–11} that ferromagnetism can be produced in semiconductor materials at room temperature through transition metal doping. All the proposed mechanisms^{5–9} for the FM ordering in DMS oxides involves oxygen vacancies and/or the resulting changes in carrier concentration. The magnitudes of the FM parameters should, therefore, vary with oxygen stoichiometry. Based on this, we believed that the FM properties of DMS oxides could be altered under suitable gaseous environments. Conversely, by monitoring changes in the FM properties of a DMS oxide, reactive gases in the sample neighborhood could be detected and their concentration estimated. This work demonstrates the systematic variation of saturation magnetization M_s , coercivity H_c , and remanence M_r of nanoscale

$\text{Sn}_{0.95}\text{Fe}_{0.05}\text{O}_2$ with the hydrogen gas flow rate.

Recently, the authors prepared FM $\text{Sn}_{1-x}\text{Fe}_x\text{O}_2$ nanoparticles using a chemical technique with sizes from 20 to 70 nm and with a Curie temperature $T_c \leq 850$ K, up to which the FM ordering continues.^{3,4} Detailed characterization studies, reported in Refs. 3 and 4, confirmed the phase purity and intrinsic origin of the observed room-temperature ferromagnetism in $\text{Sn}_{1-x}\text{Fe}_x\text{O}_2$ prepared by annealing the reaction precipitate at 350 °C. The experimental setup employed to conduct the magnetic gas sensing measurements consisted of a commercial vibrating sample magnetometer ($H \pm 15$ kOe) with a high temperature (300–1000 K) oven with options for controlled gas flow using mass flow controllers. All magnetic and gas sensing measurements on the samples employed in this work were carried out on pressed pellets firmly attached to a quartz rod. The pressed pellet form was chosen to avoid any possibility of spurious signals from loosely mounted powder samples, although this approach will reduce the actual surface area of the particles exposed to the sensing gas. To investigate the mass change response of the sample to hydrogen gas flow, a thermogravimetric analyzer (TGA) equipped with a high temperature furnace (300–1800 K) was used. X-ray diffraction (XRD) and x-ray photoelectron spectroscopy (XPS) were used to investigate both the structural and chemical stabilities of the $\text{Sn}_{0.95}\text{Fe}_{0.05}\text{O}_2$ samples in regard to the H_2 treatment.

The hysteresis loop of the fresh $\text{Sn}_{0.95}\text{Fe}_{0.05}\text{O}_2$ pellet measured in air at 300 K showed $M_s = 131$ memu/g, $H_c = 40$ Oe, and $M_r = 17$ memu/g.³ Flowing 10% hydrogen in helium gas (0–200 ml/min) through the sample chamber at 300 K as well as 375 K did not show any measurable change in the magnetic parameters. However, with further increases in the sample temperature, significant changes in the hysteresis loop parameters were observed. Figure 1(a) shows changes in M_s from the hysteresis loops measured at 575 K as a function of hydrogen flow rates. Close examination of the low field region of the hysteresis loops showed that both H_c and M_r also increase systematically with flow rate [Fig. 1(b)]. In Figs. 1(c)–1(e), the observed variation of M_s , H_c , and M_r of the $\text{Sn}_{0.95}\text{Fe}_{0.05}\text{O}_2$ pellet, as a function of H_2 flow

^{a)}Electronic mail: apunnoos@boisestate.edu

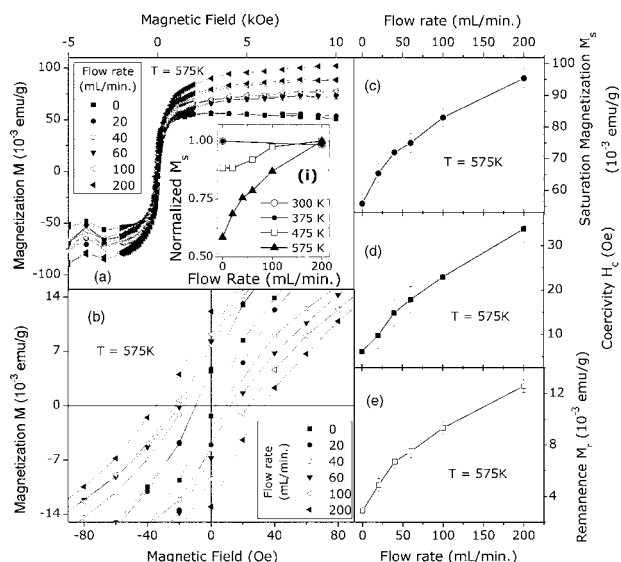


FIG. 1. Hysteresis loops of a 5% Fe doped SnO_2 pellet measured at 575 K as a function of hydrogen gas (10% H_2 in He) flow rates. (a) Full loops showing the changes in the saturation magnetization M_s . (b) Low field region of the loops showing changes in coercive field H_c and remanence M_r with increasing gas flow. (c) Changes in saturation magnetization M_s obtained by averaging the values for M_s at a field $H = \pm 10$ kOe for each flow rate (d) coercivity H_c and (e) remanent magnetization M_r . Inset (i) panel (a) illustrates the change in the M_s values as a function of the hydrogen gas flow rates at various sample temperatures.

rate measured at 575 K, is shown. These plots show that the FM parameters M_s , M_r , and H_c indeed act as gas sensing parameters and, with the appropriate calibration, can be used to detect hydrogen. The inset (i) of Fig. 1 shows the relative changes in M_s with hydrogen flow rate measured at 300, 375, 475, and 575 K. These data indicate that in order to observe the magnetic gas sensing effect, the operating temperature should be ≥ 475 K and the sensitivity of the material to the exposed gas increases with sample temperature. For this reason, all of the detailed sensing experiments reported here were performed at the optimal sample temperature of 575 K. Interestingly, such elevated operating temperatures of ≥ 475 K are also required in conventional electrical-property-based metal oxide gas sensors² to allow the chemical reduction of the gas molecules by the oxygen species on the particle surface and this results in increased carrier concentration and electrical conductivity. Also, chemisorbed water present on the particle surface at temperatures < 475 K might inhibit particle-gas interaction. Both of these factors are also expected to be important for the magnetic gas sensing process employing DMS oxide materials. The H_2 atmosphere produces oxygen vacancies in $\text{Sn}_{0.95}\text{Fe}_{0.05}\text{O}_2$ causing changes in the observed magnetic properties (Fig. 1). These results are in agreement with recent reports showing that certain DMS materials show high degrees of ferromagnetism when they are oxygen deficient.^{8,9}

Figure 2(a) shows the magnetic response characteristics of $\text{Sn}_{0.95}\text{Fe}_{0.05}\text{O}_2$ with the H_2 atmosphere. The sample magnetization increases rapidly as soon as a constant gas flow of 150 ml/min (10% hydrogen in helium) is introduced into the sample chamber. Once the H_2 flow is stopped, the magnetization of the material drops to its original value. This was done several times to verify that the effect is consistent over a period of time. These data show a clear and fast response in addition to the reversible nature of the gas induced magnetic changes of $\text{Sn}_{0.95}\text{Fe}_{0.05}\text{O}_2$, a very essential feature for practi-

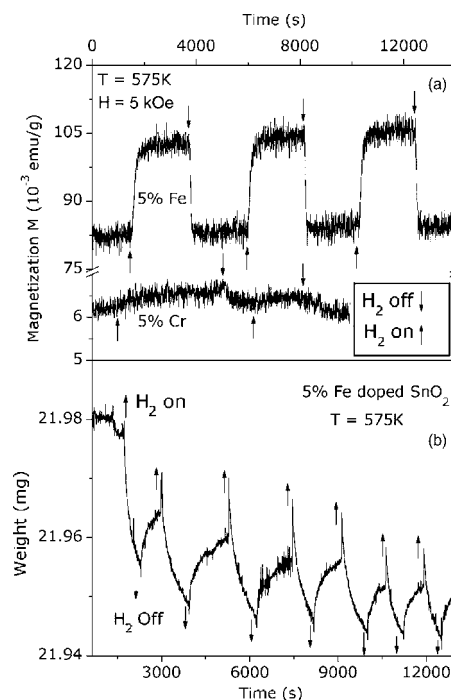


FIG. 2. (a) shows the magnetic response characteristics of both 5% Fe and 5% Cr doped SnO_2 pellets towards hydrogen (150 mL/min, 10% H_2 in He) gas flow at 575 K in an applied external field of 5000 Oe and (b) shows the weight change (TGA) as the 5% Fe doped sample is subjected to periodic H_2 atmosphere. Arrows indicate H_2 on (up) and H_2 off (down).

cal gas sensors. SnO_2 samples doped with other transition metal ions such as Co and Cr at similar concentrations (5%) were paramagnetic¹⁰ and no such gas induced magnetic changes were observed [see Fig. 2(b)]. The $\text{Sn}_{0.95}\text{Fe}_{0.05}\text{O}_2$ sample did not lose its FM behavior after successive gas sensing cycles suggesting good stability of the material. Figure 2(b) shows the change in the weight of the $\text{Sn}_{0.95}\text{Fe}_{0.05}\text{O}_2$ sample measured using the TGA system while passing a 10% hydrogen in helium mix through the sample chamber. The sample was kept at 575 K and the sample weight decreases each time the gas flow is turned on, increasing again when the flow is shut off. The data is very analogous with that of the magnetic response observed from $\text{Sn}_{0.95}\text{Fe}_{0.05}\text{O}_2$ [Fig. 2(a)]. It clearly shows that the gas flow produces the weight loss through oxygen removal and all the lost oxygen vacancies are not replenished completely after stopping the hydrogen flow. This explains the improved magnetic behavior of the sample after the gas flow experiment.

The left panel of Fig. 3 shows the XRD patterns of the sample before and after passing H_2 . The as-prepared sample primarily contains the tetragonal cassiterite form of SnO_2 along with weak traces of orthorhombic SnO_2 and tin monoxide (SnO). It was shown that Fe doping in SnO only produces paramagnetism while a FM behavior results from Fe doped SnO_2 .³ No additional peaks/phases were found in the H_2 treated sample, although some of the weak orthorhombic SnO_2 phase was converted to tetragonal cassiterite after the initial hydrogen treatment. The H_2 exposed sample showed a shift in the XRD pattern towards lower angles relative to the pattern obtained on the sample before exposure to H_2 . The magnitude of the shift correlates to an increase in lattice volume of the tetragonal SnO_2 phase from 71.3 \AA^3 (in the as-prepared sample) to 72.6 \AA^3 (in the H_2 treated sample). This indicates that the oxygen removal reduced the internal pressure which has been considered as the cause of the meta-

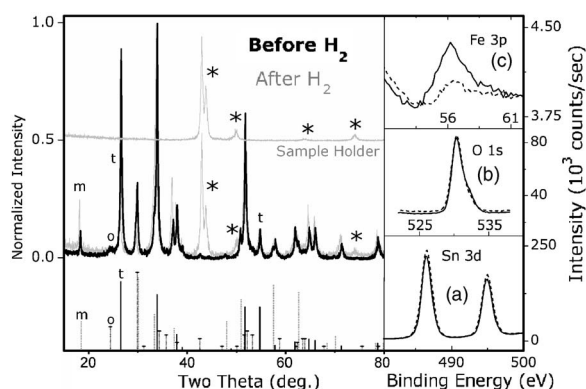


FIG. 3. Left panel shows the x-ray diffraction patterns of the 5% Fe doped SnO₂ sample before (dark line) and after (gray line) H₂ gas sensing measurements. The extra peaks observed in the H₂ treated pellet (marked with *) are from the sample holder (which appeared because the small specimen pellet could not cover the x-ray exposed area). Peaks due to monoxide SnO (marked m), orthorhombic SnO₂ (marked t), and tetragonal SnO₂ (marked o) are shown along with their reference patterns in short dash line (SnO), solid line with horizontal marker (orthorhombic SnO₂), and solid line (tetragonal SnO₂) colors for comparison. Right panel shows the room-temperature XPS data for the (a) Sn 3d, (b) O 1s, and (c) Fe 3p peaks of 5% Fe doped SnO₂ before (solid line) and after (dashed line) the H₂ treatment at 575 K.

stable orthorhombic phase formation in nanoscale SnO₂.^{10–12} This conversion happened only during the initial H₂ treatment of the sample, however, the reversible magnetic sensing behavior shown in Fig. 2(a) was observed in successive measurements without any additional change in the sample composition. Figures 3(a)–3(c) (right panels) show the XPS spectra of the sample taken before and after the H₂ treatment. The Fe 3p_{1/2} peak, which appears at 56.4 eV in the fresh sample,^{3,4} did not show any measurable shift after the H₂ gas treatment indicating that the chemical environment of the Fe ions did not change. The lack of observable shifts in this photopeak indicates that the H₂ treatment did not produce metallic iron (53.2 eV) on the particle surface. Since most iron oxides also produce Fe 3p_{1/2} peaks at lower energies than observed, the absence of change in the peak position (56.4 eV) also supports the view that other iron oxides [hematite (55.7 eV), maghemite (55.4 eV), or magnetite (53.9 eV)] were not produced to an extent that they could be observed on the surface. This shows that the observed magnetic gas sensing effect is due to changes in the oxygen environment within the Sn_{0.95}Fe_{0.05}O₂ material. The absence of any measurable shift in the binding energies of the O 1s and Sn 3d states (Fig. 3, right panel) after H₂ treatment further supports the phase stability of the sample.

In conclusion, we have shown that the magnetic properties of a DMS oxide can be used as gas sensing parameters, using FM Sn_{0.95}Fe_{0.05}O₂ as an example. The magnetic parameters M_s , M_r , and H_c of the sample are very sensitive to H₂ gas, thus providing various options to develop practical magnetic gas sensors. While more experiments are necessary to develop simpler and more convenient methods of magnetic detection, materials refinement to improve the magnetic sensitivity and response of the samples to hydrogen and other gases, and to confirm the underlying mechanism, this work provides clear experimental evidence that magnetic

functionality can be used as a gas sensing parameter. This approach defines a magnetic gas sensing process employing the magnetic property of a material, analogous to the electrical property in conventional gas sensors.

The development of DMS's has been proposed as the most important step in producing practically useful spintronics devices such as spin light emitting diodes, spin field effect transistors, and magnetic bipolar transistors, which exploit the magnetic behavior (spin) of particles in addition to their charges.^{13–15} However, prior to this research, no such device or idea employing magnetism as a gas sensing parameter has been conceived or investigated. This work, therefore, demonstrates an application of DMS's in an area that has been, until now, completely unrealized and outside of expected areas of application.^{13–15} Compared to their electrical-property-based gas sensor counterparts,^{1,2} magnetic gas sensors would be much more attractive for the following reasons. (i) No electrical contacts are required to detect a response to the gas, which allows nanoscale powder samples to be used in static as well as moving systems, such as hydrogen-powered vehicles, and when employed in the presence of reactive chemicals and/or pollutants. (ii) Prepared in the nanoparticle form, powder samples have a much larger surface area when compared to thin films and bulk crystals, providing greatly improved sensitivity. (iii) Magnetic response is much faster than electrical response.^{13–15} (iv) The operating temperature range can be as high as the T_c of the sample, in contrast to the limited operating temperature ranges of conventional gas sensors.^{1,2}

This research was supported in part by Petroleum Research Fund (PRF No. 41870-AC10), DOE-EPSCoR grant (DE-FG02-04ER46142), NSF-Idaho-EPSCoR Program (EPS-0447689), and NSF-CAREER award (DMR-0449639). A portion of the research was performed in the Environmental Molecular Sciences Laboratory, a U.S. Department of Energy user facility.

¹P. T. Moseley, *Sens. Actuators B* **6**, 149 (1992).

²R. F. Taylor and J. S. Shultz, *Handbook of Chemical and Biological Sensors* (IOP, Philadelphia, PA, 1996).

³A. Punnoose, J. Hays, A. Thurber, M. H. Engelhard, R. K. Kukkadapu, C. Wang, V. Shutthanandan, and S. Thevuthasan, *Phys. Rev. B* **72**, 054402 (2005).

⁴X. Mathew, J. Hays, C. Mejía-García, G. Contreras-Puente, and A. Punnoose, *J. Appl. Phys.* **99**, 08M101 (2006).

⁵K. Sato and H. Katayama-Yoshida, *Physica B* **308/310**, 904 (2001).

⁶T. Dietl, H. Ohno, and F. Matsukura, *Phys. Rev. B* **63**, 195205 (2001).

⁷J. Philip, A. Punnoose, B. I. Kim, K. M. Reddy, S. Layne, J. O. Holmes, B. Satpati, P. R. Leclair, T. S. Santos, and J. S. Mooder, *Nat. Mater.* **5**, 298 (2006).

⁸A. H. MacDonald, P. Schiffer, and N. Samarth, *Nat. Mater.* **4**, 195 (2005).

⁹J. M. D. Coey, M. Venkatesan, and C. B. Fitzgerald, *Nat. Mater.* **4**, 173 (2005).

¹⁰J. Hays, A. Punnoose, R. Baldner, M. H. Engelhard, J. Peloquin, and K. M. Reddy, *Phys. Rev. B* **72**, 075203 (2005).

¹¹A. Punnoose, J. Hays, V. Gopal, and V. Shutthanandan, *Appl. Phys. Lett.* **85**, 1559 (2004).

¹²B. Lu and C. Wang, *Appl. Phys. Lett.* **70**, 717 (1997).

¹³S. D. Sarma, *Am. Sci.* **89**, 516 (2001).

¹⁴N. Lebedeva and P. Kuivalainen, *J. Appl. Phys.* **93**, 9845 (2003).

¹⁵H. A. Engel, P. Recher, and D. Loss, *Solid State Commun.* **119**, 229 (2001).